Observation of the First-Order Transition in Ultrafiltration of Flexible Linear Polymer Chains

Fan Jin and Chi Wu*

The Hefei National Laboratory of Physical Science at Microscale, Department of Chemical Physics, The University of Science and Technology of China, Hefei, Anhui 230026, China

Department of Chemistry, The Chinese University of Hong Kong, Shatin, New Territories, Hong Kong

(Received 1 December 2005; published 12 June 2006)

Using a special double-layer membrane to avoid interaction among flow fields generated by different pores, we have, for the first time, observed the predicted discontinuous first-order transition in ultrafiltration of flexible linear polymer chains. Namely, the chain could pass through a pore much smaller than its unperturbed radius only when the flow rate is higher than a certain value. When only one chain and one pore are considered in theory, such a threshold is surprisingly independent of both the chain length and the pore size. Our results reveal that for a membrane with many pores and at a microscopic flow rate (q) lower than the threshold, the inevitable blocking of some pores by longer nonstretched coiled chains increases q in those unblocked pores because the macroscopic flow rate (Q) is a constant. Long chains have two populations, coiled and stretched, in a real ultrafiltration experiment when q is lower than the threshold.

DOI: 10.1103/PhysRevLett.96.237801 PACS numbers: 61.41.+e, 36.20.−r

Generally speaking, the ultrafiltration of dilute polymer solutions is mainly determined by the three following factors: (1) the deformation of flexible polymer chains under an ultrahigh velocity gradient; (2) the flow velocity field difference induced by different membrane microstructures; and (3) the interaction between polymer chains and the membrane used [1]. In theory, the conformation of a flexible linear polymer chain can change from a random coil to a stretched one under a flow velocity gradient if the product of the strain rate and the largest relaxation time of the unperturbed chain is larger than a constant (threshold). de Gennes [2] pointed out that the coil-to-stretch transition was a ''first-order'' transition under an elongational shear flow or a ''second-order'' transition under a vorticity shear flow. Anderson *et al.* [3–7] have made some significant contributions in this area of study, but no one, to our knowledge, has so far observed the first-order transition.

In a real ultrafiltration experiment, the microscopic flow velocity in each nanochannel must be much faster than the macroscopic flow velocity because the total area of the cross-section of all the pores is only a small fraction of surface area of the membrane. For each pore with a convergent type on the membrane surface, there exists a high longitudinal gradient at its entrance. Apparently, a coiled chain can pass through a pore much smaller than its unperturbed size only when it is stretched. The strain rate (ε) under an elongation gradient is related to the microscopic flux inside the pore (j) as [8]

$$\varepsilon(r) = \frac{\partial v_z}{\partial r} \approx \frac{q}{r^3} \propto \frac{d^2}{4r^3} j \tag{1}$$

where q is the microscopic flow rate inside the pore and v_z is the velocity in the direction perpendicular to the membrane surface; d is the pore diameter; and $0 < r < d/2$, a distance away from the center line of the pore. Note that the nonslip boundary condition is a precondition in the general ultrafiltration theory [8]. Theoretically, the elongation flow exists under the nonslip condition in the ultrafiltration. In reality, the boundary condition might change with the flow rate, which was not considered in previous existing theories. Later, we will show that our experimental result is consistent with the existing theory, which indicates that the boundary condition is not significantly affected by the flow rate in the current experiment. Under the nonslip boundary condition, near the wall of the pore ($r \geq d/2$), the flow velocity is approaching zero. On the other hand, near the centerline ($r \geq 0$), the flow lines align parallel to the pore axis. The threshold (ε_c) of the first-order transition is determined by [9]

$$\varepsilon_C \sim \frac{1}{\tau_{Z0}} \sim \frac{k_B T}{\eta_0 R_F^3} \tag{2}$$

where τ_{z0} is the longest relaxation time of the chain in the Zimm model; k_B is the Boltzmann constant; T is the absolute temperature; η_0 is the solvent viscosity; R_F is the unperturbed radius of the chain. The necessary condition for a flexible linear chain to pass through a much smaller pore is that the strain rate is equal to or larger than the threshold [3,8,10]. In this case, $r \sim R_F$ so that $j \geq k_B T/\eta_0 (d/2)^2$ on the basis of Eqs. (1) and (2). In principle, one could observe such a first-order transition near the threshold by increasing or decreasing the flow rate. Note that, in theory, only one pore and one chain are considered. In a real experiment, the macroscopic flux (J) is related to the number of pores (n) on a membrane and the microscopic flow flux (j) by $J \sim njd^2$. Therefore, the macroscopic threshold (J_c) is proportional to $k_B T n/\eta_0$, which should be independent of both the chain length and the pore size. To our knowledge, such a predicted on-or-off discontinuous first-order transition has not yet been ob-

served; namely, only a gradual transition was reported in literature [3,11,12]. The discrepancy between the theory and experimental results was attributed to interaction among flow fields induced by different pores; namely, the flow field is not purely elongational [12].

In order to test such an explanation, we recently used a special double-layer membrane from Whatman to block interaction among different flow fields. Figure 1 shows such a two-layer structure. The upper thick layer (A) and the under thin layer (B) contain 200 and 20 nm pores, respectively. Each large pore on average contains only one small pore. The flow fields generated at the entrances of small pores are isolated from each other. Comparing the pore size and the membrane thickness, we can regard each small pore as a one-dimensioned channel. The membrane has been well characterized before [13].

Moreover, we intentionally selected one shorter (PS-S, $M_{w,\text{PS-S}} = 3.5 \times 10^4$ g/mol and $M_w/M_n = 1.13$) and one longer (PS-L, $M_{w,\text{PS-L}} = 6.9 \times 10^6$ g/mol and $M_w/M_n = 1.06$) narrowly distributed polystyrene standards from Polymer Laboratories. The average hydrodynamic radii ($\langle R_h \rangle$) of shorter and longer chains are 9 and 99 nm, respectively. As expected, shorter polystyrene (PS-S) chains should be able to pass through the small pores without any hindrance. Therefore, these short chains act as an internal reference in our experiments when we used a mixture of the PS-S ($C_{\text{PS-S}} = 9.45 \times 10^{-3}$ g/mL) and longer polystyrene (PS-L) ($C_{\text{PS-L}} = 4.10 \times 10^{-5}$ g/mL) solutions with a volume ratio of 1:4. A syringe pump (KD Scientific) was used to accurately control the macroscopic flow rate (Q) in the ultrafiltration. Using a combination of static and dynamic laser light scattering (LLS), we are able to characterize both the absolute and relative contents of PS-S and PS-L chains in the solution mixtures before and after the ultrafiltration under different macroscopic flow rates.

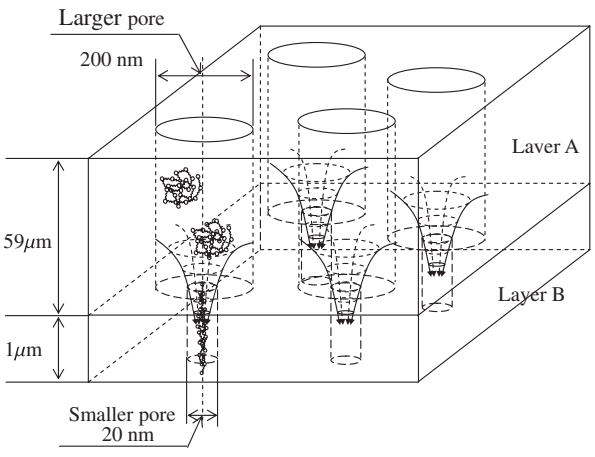

FIG. 1. Passing of flexible linear polymer chain with double-layer membrane (Whatman) in ultrafiltration (not in a proportional scale).

In dynamic LLS, we measured the photon correlation function [$G^{(2)}(\tau)$] of each solution before and after the ultrafiltration. $G^{(2)}(\tau)$ is related to the electric filed correlation function [$g^{(1)}(\tau)$] [14,15]. The Laplace inversion of each $g^{(1)}(\tau)$ leads to a line-width distribution [$G(\Gamma)$] [15], which can be further converted to a hydrodynamic radius distribution [$f(R_h)$] by using the Stokes-Einstein equation, as shown in Fig. 2. Each of the two peaks comes from one PS standard in the solution. The area under each peak (A) is proportional to the time-averaged intensity of the light scattered from one PS standard. Therefore, the area ratio of the two peaks (A_s/A_L) equals the ratio of the scattered light intensities (I_S/I_L) of PS-S and PS-L in the solution mixture. On the other hand, in static LLS, I_S and I_L are proportional to the molar masses (M) and concentrations (C) of PS-S and PS-L, respectively; i.e., [15]

$$A_S/A_L = I_S/I_L = C_S M_S / C_L M_L \tag{3}$$

and the total time-averaged scattered light intensity ($\langle I \rangle$) of the solution mixture at infinite dilution solution and the zero scattering angle equals the sum of I_s and I_L, i.e., [15]

$$\langle I \rangle = (I_S + I_L) = K(C_S M_S + C_L M_L) \tag{4}$$

where K is a constant for a given type of polymer and solvent. The left sides of Eqs. (3) and (4) can be measured from dynamic and static LLS, respectively. For a given solution mixture, K, M_S, and M_L are three known constants. C_S and C_L can be calculated from Eqs. (3) and (4).

Figure 3 shows that for a given microscopic flow rate ($q = 3.5 \times 10^{-12}$ cm^3/s and the estimated Deborah number), both $\langle I \rangle$ and A_S/A_L are independent of the filtration time. It reveals that under such a flow rate both shorter PS-S and longer PS-L chains can pass through the 20 nm

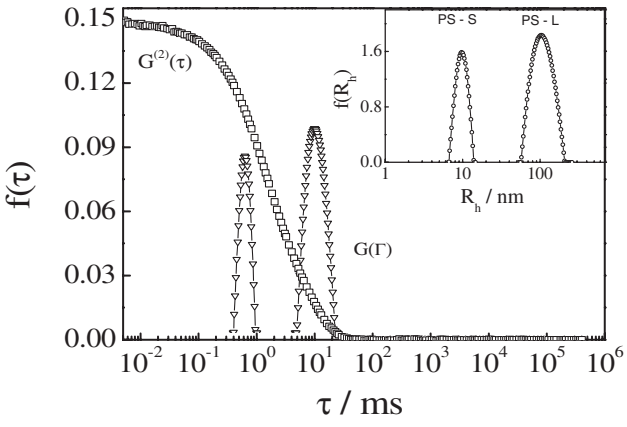

FIG. 2. Intensity-intensity time correlation function $G^{(2)}(\tau)$ of the solution mixture and its related line-width distribution $G(\Gamma)$ calculated from the Laplace inversion of the measured $G^{(2)}(\tau)$. The inset shows the hydrodynamic radius distribution $f(R_h)$ calculated from $G(\Gamma)$ by using the Stokes-Einstein equation.

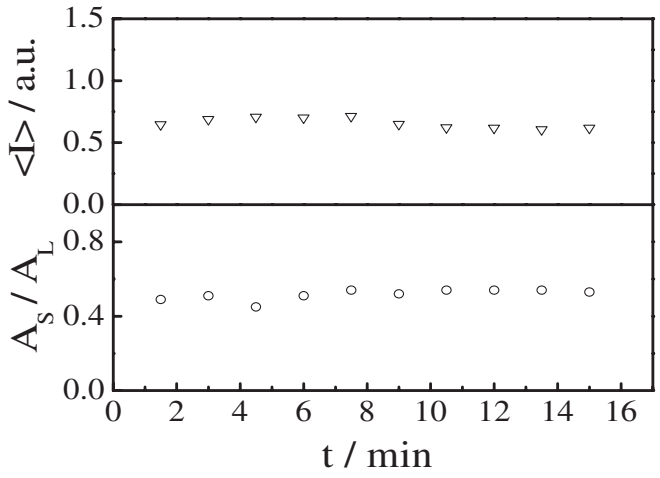

FIG. 3. Time dependence of the average scattered light intensity ($\langle I \rangle$) and the area ratio of the two peaks (A_S/A_L) in line-width distribution $G(\Gamma)$ during ultrafiltration of the solution mixture of PS-S and PS-L.

pores, just as if these pores did not exist. However, the situation completely changes when we decrease q, as shown in Fig. 4. An abrupt increase of A_S/A_L and an abrupt decrease of $\langle I \rangle$ are observed when q is lower than 4.4×10^{-14} cm^3/s (the estimated Deborah number is $\sim$0.72. The facts that short chains with a size smaller than the pore can pass the membrane at any flow rate and that long chains can only pass through the pores at high flow rates indicate that the flow is more likely elongational.

A combination of A_S/A_L and $\langle I \rangle$ leads to C_S and C_L in the solution mixture after the ultrafiltration. To have a better view, we can express them as the retention value $((C_{S,0} - C_S)/C_{S,0}$ or $(C_{L,0} - C_L)/C_{L,0})$, i.e., the percentage of short ($\lambda = 0.9$) or long chains ($\lambda = 9.9$) which were not able to pass the membrane during the ultrafiltration, as shown in Fig. 5, where λ is the radius ratio of the chain (R_h) and the pore ($d/2$). For comparison, we also summarized and plot the data from Anderson *et al.* [12] in Fig. 5. It is clear that as q decreases, one is a gradual transition and another is an abrupt transition.

Moreover, the inset of Fig. 4 shows that the peak related to long PS-L chains shifts to the left by $\sim$14 nm when q is lower than the threshold. Note that such a shift is much larger than the experimental uncertainty (1–2 nm). It reveals that some of longer PS-L chains cannot pass through the pores. This is contrary to the prediction that the threshold should be independent of both the chain length and the pore size. How to explain such a discrepancy? Note that only a single pore and a single chain are considered in theory in which there are only two opposite situations: passing or not passing. In a real ultrafiltration experiment, there are many pores on the membrane and many chains in the solution. When the macroscopic flux is lower than the threshold, the flow field cannot stretch some of longer PS-L chains at the entrance of small pores so that they start to block them. This increases the microscopic flux (j) in those unblocked pores because the macroscopic flux (J) is a constant in each of our experiments. In other words, $J = jn^*$, where n^* is the number of unblocked pores. The decrease of n^* must increase j. Therefore, even the macroscopic flow rate is lower than the threshold, but the microscopic flow rate in those unblocked pores can become higher than the threshold. This explains why long PS-L chains can apparently pass the membrane even when the macroscopic flux is lower than the threshold. We can consider that there are two populations (stretched and coiled chains) of long PS-L chains in a real ultrafiltration experiment when the macroscopic flux is lower than the threshold.

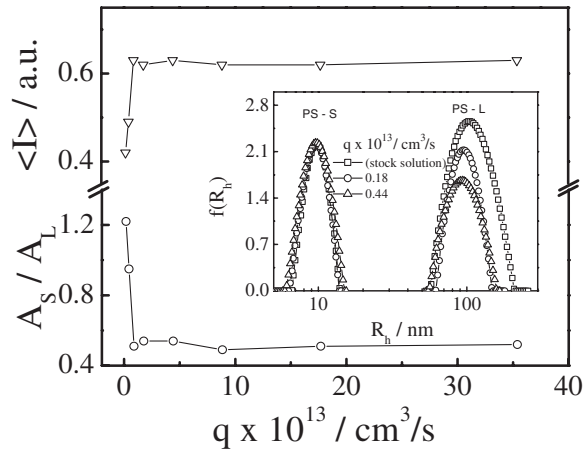

FIG. 4. Microscopic flow rate (q) dependence of averaged scattered light intensity ($\langle I \rangle$) and area ratio of the two peaks (A_S/A_L) in line-width distribution $G(\Gamma)$. The inset shows the flow rate (q) dependence of hydrodynamic radius distribution [$f_{(R_h)}$], where q is lower than the microscopic threshold flow rate (4.4×10^{-14} cm^3/s).

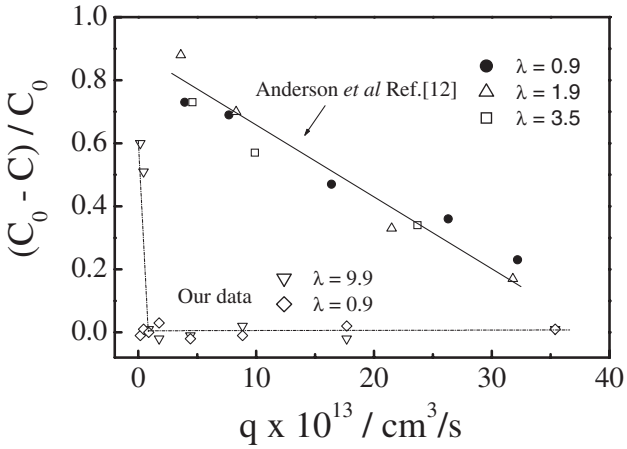

FIG. 5. Microscopic flow rate (q) dependence of retention percentage $(C_o - C)/C_o$. For comparison, we also summarize and plot some results from Anderson *et al.* [12] and list the radius ratio of the chain and pore (λ).

In summary, after preventing interaction among flow fields generated by different pores with a special double-layer membrane, we have, *for the first time*, observed the predicted discontinuous first-order transition. Namely, flexible linear polymer chains can pass through pores much smaller than their unperturbed radius only when the flux is higher than a threshold. Moreover, our results reveal that in a real ultrafiltration experiment, some of long chains are still able to pass the membrane even when the macroscopic flux is lower than the threshold. This is because that we are not dealing with only one single pore and one single chain as predicted by theory. When the macroscopic flux is lower than the threshold, some of the pores can be blocked so that the microscopic flow rate in those unblocked pores becomes higher than the threshold. There are two populations of long chains, namely, coiled chains at the entrances of the blocked pores and stretched chains passing through those unblocked pores. Note that without the two populations, the percentage of retention, $(C_o - C)/C_o$, should goes up to 100% when the macroscopic flow rate (Q) is lower than the threshold.

The finance support of the Hong Kong Special Administration Region Earmarked Grants No. (CUHI4029/03P, 2160206), the Chinese Academy of Sciences Special Grant No. (KJCX2-SW-H14) and the Natural National Science Foundation Project No. (20574065) is gratefully acknowledged.

*The Hong Kong address should be used for all corresponding.

[1] S. Daoudi and F. Brochard, Macromolecules **11**, 751 (1978).
[2] P. G. de Gennes, J. Chem. Phys. **60**, 5030 (1974).
[3] J. A. Quinn, J. L. Anderson, W. S. Ho, and W. J. Petzny, Biophys. J. **12**, 990 (1972).
[4] D. M. Malone and J. L. Anderson, AIChE J. **23**, 177 (1977).
[5] J. L. Anderson and J. A. Quinn, Biophys. J. **14**, 130 (1974).
[6] J. L. Anderson, J. Theor. Biol. **90**, 405 (1981).
[7] T. D. Long and J. L. Anderson, J. Polym. Sci. **23**, 191 (1985).
[8] Quang Trong Nguyen and Jean Neel, J. Membr. Sci. **14**, 111 (1983).
[9] Malika J. Menasveta and David A. Hoagland, Macromolecules **25**, 7060 (1992).
[10] M. A. M. Beerlage, M. L. Heijnen, M. H. V. Mulder, C. A. Smolders, and H. Strathmann, J. Membr. Sci. **113**, 259 (1996).
[11] David S. Cannell and F. Rondelez, Macromolecules **13**, 1599 (1980).
[12] T. D. Long and J. L. Anderson, J. Polym. Sci. **22**, 1261 (1984).
[13] Fan Jin and Chi Wu, Acta Polym. Sinica **4**, 486 (2005).
[14] B. Berne and R. Pecora, *Dynamic Light Scattering* (Plenum Press, New York, 1976).
[15] B. Chu, *Laser Light Scattering* (Academic Press, New York, 1991), 2nd ed.